Taylor & Francis
Taylor & Francis Group

RESEARCH ARTICLE

Jiedutongluotiaogan formula restores pancreatic function by suppressing excessive autophagy and endoplasmic reticulum stress

Jinli Luo[a], Wenqi Jin[b], Meiying Jin[c], Weiwei Pan[d], Shengnan Gao[a], Xiaohua Zhao[a], Xingrong Lai[a], Liwei Sun[b] and Chunli Piao[a]

[a]Institution of Shenzhen Hospital, Guangzhou University of Chinese Medicine (Futian), Shenzhen, China; [b]Research Center of Traditional Chinese Medicine, the Affiliated Hospital to Changchun University of Chinese Medicine, Changchun, China; [c]The Third Affiliated Hospital to Changchun University of Chinese Medicine, Changchun, China; [d]School of Clinical Medicine, Changchun Medical College, Changchun, China

ABSTRACT

Context: Jiedutongluotiaogan formula (JTTF), a traditional Chinese medicine (TCM), could promote islet function. However, the potential effect of JTTF on endoplasmic reticulum stress (ERS) and autophagy have not been reported.

Objective: This study explores the potential effect of JTTF on ERS and autophagy in the pancreas.

Materials and methods: The Zucker diabetic fatty (ZDF) rats were randomised into five groups, control, model, JTTF (1, 3, 5 g/kg/day for 12 weeks). LPS induced pancreatic β-cells were treated with JTTF (50, 100, 200 μg/mL). LPS was used to induce pancreatic β-cell injury, with cell viability and insulin secretion evaluated using MTT, glucose-stimulated insulin secretion (GSIS) assays, and PCR. Intracellular Ca^{2+} concentration was measured using flow cytometry, while ERS and autophagy levels were monitored via Western blotting and/or immunostaining.

Results: Compared with the model group, body weight, FGB, HbA1c, IPGTT, FINs, and HOMA-IR in JTTF treatment groups were significantly reduced. In islets cells treated with JTTF, the pancreatic islet cells in the JTTF group were increased, lipid droplets were reduced, and there was a decrease in Ca^{2+} (16.67%). After JTTF intervention, PERK, p-PERK, IRE1α, p- IRE1α, ATF6, eIF2α, GRP78, p-ULK1, LC3 and p62 expression decreased, whereas Beclin1and p-mTOR expression increased. In addition, the expression of proteins related to apoptosis in the JTTF groups were lower than those in the control group.

Discussion and conclusions: JTTF may alleviate pancreatic β-cell injury by inhibiting ER stress and excessive autophagy in diabetic rats. This provides a new direction for treating diabetes and restoring pancreatic dysfunction by TCM.

Introduction

Diabetes mellitus (DM), a group of metabolic disorders characterised by increased blood glucose concentration, is a chronic lifestyle-induced condition that affects millions of people worldwide. According to the International Diabetes Foundation (IDF), 415 million people have been diagnosed with diabetes worldwide, a number that is projected to increase to over 600 million people by 2040 (Ogurtsova et al. 2017). In 2017, around 5 million people died due to diabetes, and 850 million dollars were spent on diabetic care, which led to serious financial burdens (Cho et al. 2018). Generally, inflammatory pathways have been implicated as underlying mediators of common pathogenic disorders, such as obesity and DM (Shoelson et al. 2006). The long-term low and chronic inflammation damages the pancreatic β-cells and decreases insulin secretion, which leads to hyperglycaemia (Berbudi et al. 2020). Previous research has shown that the levels of inflammatory biomarkers are correlated with prevalent and incident diabetes, as well as with major diabetic complications and cardiovascular diseases (Lontchi-Yimagou et al. 2013). Meanwhile, endoplasmic reticulum stress (ERS) has been shown

to be one of the key pathogenic processes to β-cell dysfunction and death associated with DM development (Lei and Davis 2003; Ozcan et al. 2006). Notably, an accumulating body of research has increasingly demonstrated that autophagy promotes β-cell survival by postponing apoptosis, as well as alleviates negative impacts of ERS and DNA damage (Hayes et al. 2017).

Autophagy, as a lysosomal degradation process (Wang et al. 2017), is an important process for maintaining homeostasis and can promote cell survival following cellular stress and starvation (Hashemzaei et al. 2017). Under conditions of nutritional deficiencies, induction of autophagy stimulate cells to reuse their own constituents for energy (Song et al. 2015). However, excessive activation of autophagy results in unconscionable self-digestion and degradation of cells that may trigger autophagic cell death (Sciarretta et al. 2018). In one study using a diabetic model based on palmitic acid (PA)-induction of cell insulin resistance (IR) in cardiomyocytes (Li et al. 2017), development of IR was shown to be accompanied by excessive autophagic activation and increased apoptosis. Meanwhile, excessive autophagy has been linked to ERS, the unfolded protein response (UPR), and cell death (Liao et al. 2019). Therefore, the prevention of excessive

CONTACT Liwei Sun ✉ sunnylilwei@163.com 📍 1478 Gongnong Road, Changchun, Jilin, 130012, China; Chunli Piao ✉ pcl2013@sina.cn 📍 No. 6001, Beihuan Avenue, Futian District, Shenzhen, Guangdong, 518000, China

autophagy may be a treatment for alleviating pancreatic dysfunction. In fact, an increasing number of studies have revealed the pathogenesis of DM is multifactorial, which ERS and autophagy are essential in the development of β-cell dysfunction (Watada and Fujitani 2015). Therefore, the collective evidence warrants the development of therapies aimed at promoting β-cell repair through alleviation of ERS and excessive autophagy as therapies with great potential to provide clinical and economic benefits.

AMPK plays an important role in regulating the energy metabolism of almost all cells (Hardie 2011). The AMPK/mTOR signalling pathway is involved in the regulation of autophagy (Lamm et al. 2019). Previous research has demonstrated that AMPK could promote the occurrence of autophagy by suppressing mTOR (Kim et al. 2011; Alers et al. 2012). In addition, CaMKK could trigger AMPK phosphorylation and self-activation via the Ca^{2+}/CaMKKβ pathway (Xiao et al. 2013). The increasing intracellular Ca^{2+} concentration may lead to activation of AMPK by CaMKKβ (Cheng et al. 2004; Green et al. 2011). Ca^{2+} is a key signal factor of CaMKK in cellular, and disruption of Ca^{2+} homeostasis will trigger ERS (Liu et al. 2020). CaMKKβ/AMPK is an important signalling pathway to connect ERS and autophagy (Feng et al. 2020). In this study, JTTF was a negative regulator of ERS and excessive autophagy by regulating the CaMKKβ/AMPK signalling pathway to protect β-cell function under inflammatory conditions. Thus, we aimed to explore the effect of JTTF on ERS and autophagy of β cells and possible protective mechanisms whereby JTTF prevented β-cell damage under inflammatory conditions.

TCM describes diverse treatments with activities with multi-component, multi-target, and multi-effect modes of action. TCM formulations are composed of at least two herbs containing numerous chemical components have been selected to exert multiple effects with low toxicity and few adverse effects, such as Dangguibuxue decoction, Xiexin decoction, and Sini decoction (Ren et al. 2017; Leng et al. 2020; Wang et al. 2020; Liu et al. 2021). Due to these characteristics, TCM holds promise for use in treating T2DM and its complications. In fact, numerous studies have already shown that diverse TCMs have been successfully used to treat various diseases, including diabetes (Dai et al. 2020), with Jiedutongluotiaogan formula (JTTF) is currently prescribed as a TCM treatment with demonstrated efficacy in vivo and in vitro. JTTF could improve IR, lower blood sugar, regulate lipid metabolism, and reduce weight in obese patients with type 2 diabetes (Jin et al. 2020; Jiang et al. 2018). Furthermore, the addition of JTTF to INS-1 and HepG2 cell cultures stimulated cellular mRNA-level and protein-level expression leading to enhanced production of IRS1, Akt, and PI3K, which could improve glucose metabolism to treat diabetes (Zhang et al. 2021). Moreover, previous studies have demonstrated that some JTTF components can lower blood glucose, attenuate IR, and relieve oxidative stress (Huang et al. 2008; Jia et al. 2019; Xiong 2020).

Materials and methods

Reagents

INS-1 cells were purchased from the Cell Bank of Type Culture Collection of Chinese Academy of Sciences (Shanghai, China). Foetal bovine serum (FBS; 16000-044) and RPMI-1640 culture medium were purchased from Hyclone (Logan, UT). Primary antibodies against PDX1, PERK, IRE1α, ATF6, GRP78, CaMKKβ, p-CaMKKβ, AMPK, p-AMPK, mTOR, p-mTOR,

Table 1. The Chinese herb drugs contained in Jiedutongluotiaogan Formula.

Latin name	Weight (g)	Batch numbers
COPTIDIS RHIZOMA	15	200305
RHEI RADIX ET RHIZOMA	6	191127
SCUTELLARIAE RADIX	15	200109
SALVIAE MILTIORRHIZAE RADIX ET RHIZOMA	15	200204
BUPLEURI RADIX	10	200316
LONICERAE JAPONICAE FLOS	10	191223
POLYGONI CUSPIDATI RHIZOMA ET RADIX	10	191218

ULK1, p-ULK1, p62, Beclin 1, LC3, TNF-α, IL-1β, IL-6, Bax, Bcl-2, CASPASE3, GAPDH, and β-tublin were purchased from Cell Signalling Technology, Inc. (Danvers, MA, USA), as were secondary antibodies against rabbit immunoglobulin G (IgG) (STAR208P) and mouse IgG (STAR117P). Flou-4 AM, acridine orange (AO) dye, and ELISA kits were purchased from Shanghai Beyotime Biotechnology Co., Ltd. (Shanghai, China). Total protein of treated cells was prepared using RIPA lysis buffer (Beijing Solarbio Science & Technology Co. Ltd., Beijing, China). Protein concentration was determined using a BCA protein quantitation kit (Thermo Co. Ltd., MA).

Preparation of the JTTF extract

JTTF is composed of seven different types of medicinal herbs, with ingredients and batch numbers listed in Table 1. The mixture was refluxed with water (1:10, w/v) for 2 h then was filtered. Filtrates were collected, dried, and refluxed in water (1:10, w/v) for 1.5 h followed by pooling of two batches of filtrates. Afterwards, the concentrated extract was dried by vacuum concentration to obtain the JTTF extract at a yield of 22.3% (w/w, dried extract/crude herb). The extract was ground into powder and stored in a sealed container at 4 °C. Each HPLC standard was accurately weighed and added to a 30% methanol solution to prepare a mixed standard solution, which was diluted before use. After precise weighing of JTTF, 30% methanol was added to generate a solution. After sonication in an ice water bath for 10 min, the volume was adjusted to 25 mL. Finally, each sample was filtered through a 0.22 μm filter membrane and components were detected using a previous HPLC method (Liao et al. 2016).

Animal interventions

Forty male Zucker diabetic fatty (ZDF) rats (ZDF fa/fa/ZDF fa/+) and 10 Zucker lean rats (ZL) at the age of 8 weeks were acquired from the Beijing Vital River Laboratory Animal Technology Co., Ltd. ZDF fa/fa rats (n = 40) were used after administration with a HFD for 12 weeks. The high-fat diet Purina #5008 was provided by the Shanghai Jiehong Trading Co., Ltd. Animals were randomly divided into 5 groups (10 animals/group): the control group (ZL rats); the model (DM) group (ZDF fa/fa rats); the low-dose JTTF group (1 g/kg/day); the medium-dose JTTF group (3 g/kg/day); and the high-dose JTTF group (5 g/kg/day). Animals were anaesthetized with an intraperitoneal administration of sodium pentobarbital (50 mg/kg) and sacrificed. All experiments were reviewed and approved by the Animal Care and Welfare Committee of Changchun University of Chinese Medicine (permit number: SCXK 2014-0003).

Biochemical measurements

After 12 weeks of intervention, blood samples were extracted via tail vein puncturing. FBG was detected by a blood glucose metre

(ACCU-CHEK® Performa; Roche Co., Ltd., Shanghai, China). For each rat, body weight was measured after 2, 4, 6, 8, 10, and 12 weeks of treatment. For IPGTTs, rats were fasted overnight and given an intraperitoneal injection of glucose (2 mg/g body weight; Sigma, G7021). Glucose concentrations were measured at 0, 15, 30, 60, 90, and 120 min by using a blood glucose metre. The serum was collected for the measurement of TC, TG, LDL, HDL levels, fasting serum insulin (FINs), and HbA1c. The IR index was calculated using the homeostasis model assessment-insulin resistance (HOMA-IR) method (Liu et al. 2015).

Microstructure analysis

After rats were sacrificed, the pancreas was preserved in 10% neutral formaldehyde. Sections (4 μm-thick) of paraffin-embedded tissues were stained with haematoxylin and eosin (H&E). OCT-embedded frozen liver sections (10 μm-thick) were stained with H&E and Oil red. The pancreas pathological sections were examined under a 200-fold and liver pathological sections were examined under a 20-fold inverted fluorescence microscope (Hussain et al. 2021).

Cell culture and cell viability assay

INS-1 were cultured in RPMI-1640 culture medium containing 10% FBS with 1% (w/v) each of penicillin and streptomycin. INS-1 cells were cultured at 37 °C in a humidified atmosphere with 5% CO_2. The medium was renewed once every two days and cells were passaged every 3 to 5 days. Investigating different concentrations of JTTF to detect its toxicity of INS-1 cells, including 12.5, 25, 50, 100, 200, 400, and 600 μg/mL. To examine the effect of different concentration JTTF on the cell viability of INS-1 cells pre-treated with LPS (1 μg/mL) to simulate inflammatory conditions, a 3-(4,5-dimethylthiazol-2-yl)-2,5-diphenylte-trazolium bromide (MTT) assay was conducted. INS-1 cells were seeded at 96-well plate at 1×10^4 cells/well. After 72 h, INS-1 cells in seven groups received various treatments. After 24 h of treatment, each well was stained with 20 μL MTT solution for 4 h at 37 °C. Next, the medium was removed from each well then purple formazan crystals were dissolved in 150 μL DMSO for 10 min and the absorbance was measured at 490 nm with a microplate reader.

Glucose-stimulated insulin secretion (GSIS)

INS-1 cells were cultured at a density of 1×10^5 cells/well in a 6-well plate. 72 h after seeding, LPS plus various concentrations of JTTF were added to the cultures in each well. After a further 24 h of incubation, supernatants from each well were collected. The insulin content of culture supernatants was determined using an insulin ELISA kit according to the manufacturer's instructions (Beyotime Biotechnology, Shanghai).

Elisa

The serum was collected were collected after treatment and used to measure cytokine secretion including interleukin-6 (IL-6), interleukin-1β (IL-1β), and tumour necrosis factor-α (TNF-α) using a commercial ELISA kit according to the manufacturer's instructions (Raybiotech, USA).

Intracellular Ca^{2+} measurement by flow cytometry

INS-1 cells were cultured at a density of 1×10^5 cells/well in a 6-well plate. 72 h after seeding, LPS plus various concentrations of JTTF were added to the culture wells. After 24 h of incubation, each well was washed three times with PBS. Fluo-4AM, a calcium indicator that exhibits an increase in fluorescence upon binding Ca^{2+}, was used to detect changes in intracellular Ca^{2+} concentration. After cells were treated as mentioned above, Fluo-4AM (1.0 μM) was added followed by incubation at 37 °C in the dark for 30 min then cell fluorescence was monitored with a flow cytometer set to an excitation wavelength of 488 nm.

RT-PCR analysis

Total RNA was extracted from treated INS-1 cells with TRIzol reagent (Invitrogen, Grand Island, NY)). In short, equal RNA levels (0.5 μg) from each sample were reversed and transcribed into cDNA using HiScriptQ RT SuperMix for qPCR (TaKaRa, Tokyo, Japan). The qPCR of specific primers was analysed on the Applied Biosystems 7900 Real-Time PCR system (Applied Biosystems, Foster City, CA). The sequences of primer pairs were as follows: INS1 (forward) 5′-TAGTGACCAGCTATAA TCAGAG-3′ and (reverse) 5′-ACGCCAAGGTCTGAAGGTCC-3′; INS2 (forward) 5′-CACCAGCCCTAAGTGATCC-3′ and (reverse) 5′-CAGTAGTTCTCCAGCTGGTAG-3′; PDX1 (forward) 5′-CCTTCGGGCCTTAGCGTGTC-3′ and (reverse) 5′-CG CCTGCTGGTCCGTATTG-3′; MafA (forward) 5′-ATCATCACT CTGCCCACCAT-3′ and (reverse) 5′-TGGAGCTGGCACTTCT CGCT-3′; GADPH (forward) 5′-CCATGTTCGTCATGGGTGT GAACCA-3′ and (reverse) 5′-GCCAGTAGAGGCAGGGATGA TGTT C-3′.

Acridine orange staining (AO)

AO staining is a quick, accessible and reliable method to assess the volume of AVOs, which increase upon autophagy induction (Thomé et al. 2016). INS-1 cells were seeded into 96-well culture plates at 2×10^4 cells/well at 37 °C in a 5% CO_2 incubator. Seventy-two hours after seeding, LPS plus various concentrations of JTTF was added to the cultures in each well. After 24 h treatment, cells were washed three times with PBS, fixed with 4% formaldehyde, and permeabilized with 100% methanol. AO dye was added to cells at a final concentration of 1 μg/mL and incubated in the dark at room temperature for 15 min. Then cells were washed with PBS and visualised using a laser scanning confocal microscope (Olympus FluoView FV1000, Tokyo, Japan).

Western blot analysis

Pancreatic tissues or INS-1 cells were collected and lysed in RIPA buffer containing phosphatase inhibitor. After centrifugation for 15 min at 4 °C, cellular proteins were separated via SDS-PAGE (10–12% polyacrylamide, each gel loaded 30 μg of protein) then were transferred to polyvinylidene difluoride (PVDF) membranes. PVDF membranes were blocked with 5% non-fat milk and incubated overnight with a specific primary antibody overnight at 4 °C, and were incubated with secondary antibodies for 2 h at room temperature. Protein signals on membranes were detected using an ECL detection system.
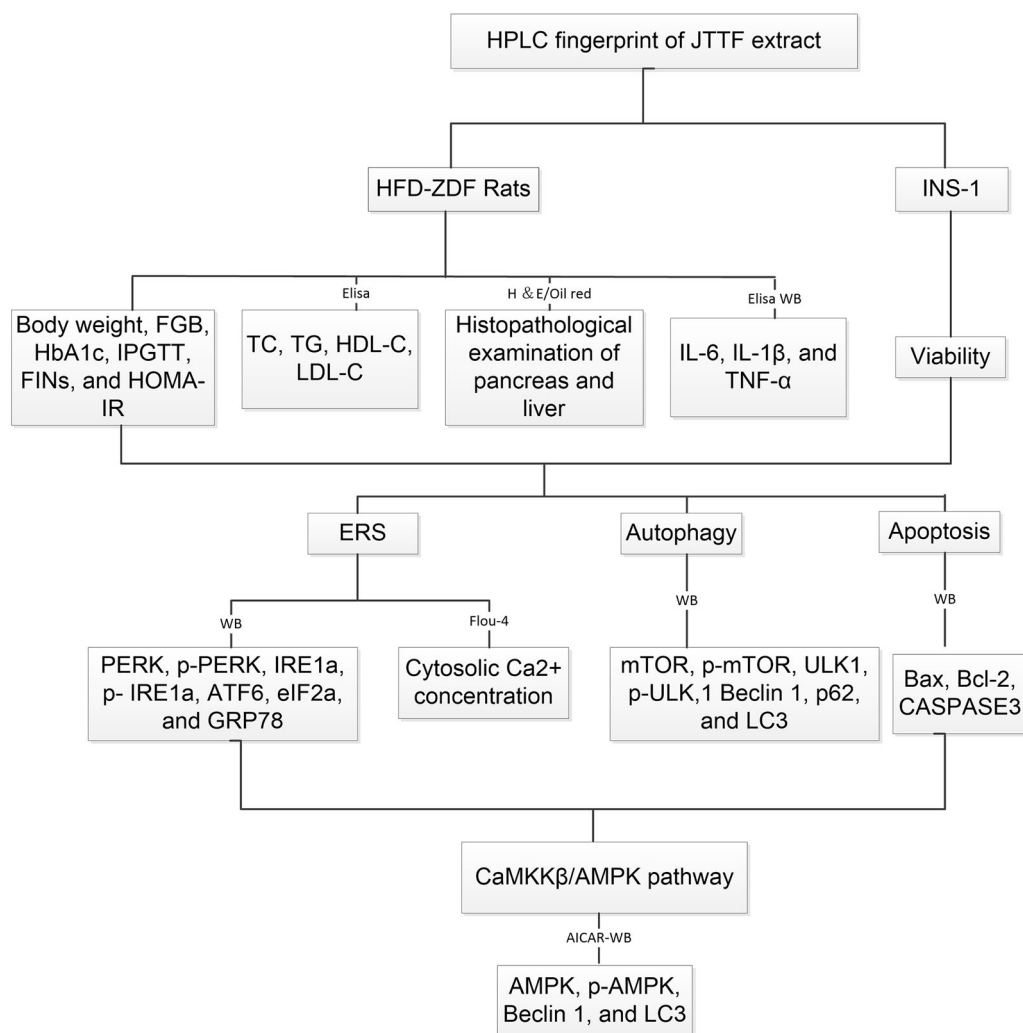
Figure 1. Flow diagram of the research based on *in vitro* and *in vivo* studies.

Statistical analysis

Data were presented as the mean ± standard deviation (SD) using IBM SPSS Statistics for Windows, version 22.0 (IBM Corp., Armonk, NY). Comparisons within two groups were made by Student's t-test. Comparisons within multiple groups were determined using ANOVA followed by Dunnett's test. Comparison with $p < 0.05$ was considered statistically significant. A flow diagram of the research is shown in Figure 1.

Results

Qualitative analysis of the chemical constituents of JTTF

HPLC fingerprinting of JTTF was conducted according to a previously reported method and generated as shown in Figure 1. Chlorogenic acid, calycosin-7-glucoside, salvianolic acid B, haragoside, and aloe-emodin were used as surrogate markers (Figure 2(a)). Five major peaks of JTTF extract were identified on the HPLC fingerprints and 5 peaks were identified (Figure 2(b)). Previous studies have reported that salvianolic acid B and aloe-emodin are the key active ingredients of Radix Salviae and Radix Rhei Et Rhizome respectively in the treatment of diabetes (Dong et al. 2020; Shi et al. 2020).

JTTF improved blood glucose and metabolic parameters in HFD-induced ZDF rats

After a 12-week HFD feed, the ZDF rats showed a higher body weight compared with the control group (Figure 3(a)). JTTF treatment could decrease body weight at all tested concentrations, with the greatest effect observed for the JTTF-H group. As shown in Figure 3(b), the FBG level in T2DM animals were greater than the control group. Treatment with 1, 3, or 5 g/kg/day JTTF decreased the elevation of FBG level compared with the T2DM group. Similarly, the HbA1c ratio, IPGTT, FINs level, and HOMA-IR were decreased by the administration of JTTF (Figure 3(c–f)). Moreover, increased serum levels of TG, TC and LDL-C and reduced HDL-C could be ameliorated by JTTF treatment (Figure 4). Therefore, JTTF could alleviate glucose and lipid metabolism disorder in ZDF rats.

JTTF reduces pancreas injury in ZDF rats

As shown in Figure 5(a), compared with the normal group, the pancreatic islet cells in the endocrine area showed irregular shape, the boundary between islet cells and acinus was blurred, the islet cells were atrophic and distributed unevenly, and more local nuclear necrosis and lysis were observed in model group.
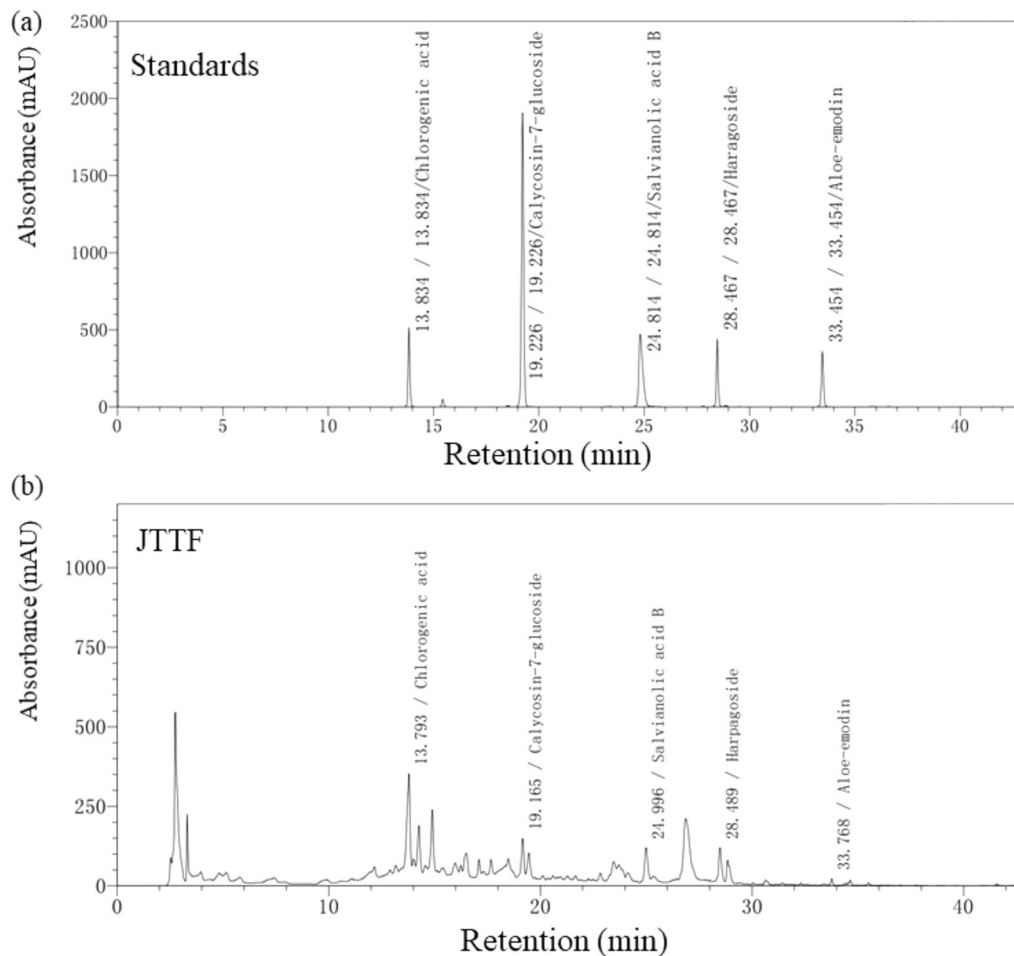
Figure 2. HPLC fingerprint of JTTF extract. (a) HPLC chromatograms of chlorogenic acid, calycosin-7-glucoside, salvianolic acid B, haragoside, and aloe-emodin with UV detection at 254 nm are shown. (b) HPLC chromatogram of JTTF with UV detection at 254 nm is shown. HPLC: high performance liquid chromatography.

Compared with the model group, the pancreatic islet cells in JTTF-H group were distributed in a mass, with clear and intact edges, and intact nuclei and exocrine acinus were irregular polygonal, neatly arranged, and the boundary among acinus was clearly visible. In the JTTF-M groups, the above pathological conditions were also improved. As shown in Figure 5(b,c), compared with the normal group, hepatocyte swelling, steatosis with lots of intercellular vacuoles, and infiltration of inflammatory cells were observed in model group. Compared with the model group, the degree of hepatocyte steatosis and the number of intercellular vacuoles in JTTF-H and JTTF-M groups were both significantly reduced, and hepatocytes were normal in size, orderly, and clear in structure.

JTTF protected pancreatic β cells and ameliorated GSIS damage

To examine the cytoprotective role of JTTF, INS-1 cells were treated different concentrations (12.5–200 μg/mL) of JTTF to assess JTTF cytotoxic effects. As shown in Figure 6, INS-1 cells cultured for 24 h with LPS to simulate inflammation exhibited reduced cell proliferation. Exposure of cells to various JTTF concentrations led to a concentration-dependent cytoprotective effect; all JTTF concentrations, (12.5, 25, 50, 100, and 200 μg/mL) promoted proliferation of INS-1 cells, with a JTTF concentration of 200 μg/mL exerting the greatest effect (Figure 6(a)).

Then, we investigated the effects of JTTF on insulin secretion by injured INS-1 cells by using an ELISA kit. LPS exposure reduced INS-1 cell insulin content, while JTTF treatment exerted a potent insulinotropic effect on INS-1 cells (Figure 6(a)). The level of insulin secretion by INS-1 cells after treatment with JTTF at all tested concentrations was increased as compared to that of the LPS-only group, with the greatest effect observed for 200 μg/mL JTTF (Figure 6(b)). PDX1, a homeodomain transcription factor, is required for early embryonic development of the pancreas (Stoffers et al. 1997). In mature beta-cells, depletion and reduction of PDX1 induces glucose intolerance as evidence for a critical role of PDX1 for maintaining beta-cell function (Holland et al. 2002). Our preliminary results showed that JTTF treatment could restore PDX1 expression levels (Figure 6(c)). The expression of mRNA of PDX1, MafA, INS1 and INS2 were upregulated in all four groups (Figure 6(d–g)).

JTTF decreased the expression of proinflammatory cytokine and chemokine in HFD rats

To further investigate the effects of JTTF on inflammatory factors, IL-6, IL-1β, and TNF-α were measured using an ELISA kit. As shown in Figure 7, JTTF treatment exerted a potent anti-inflammatory effect on HFD ZDF rats. In addition, JTTF treatment could decrease IL-6, IL-1β, and TNF-α expression levels after treatment with JTTF at all tested concentrations, with the
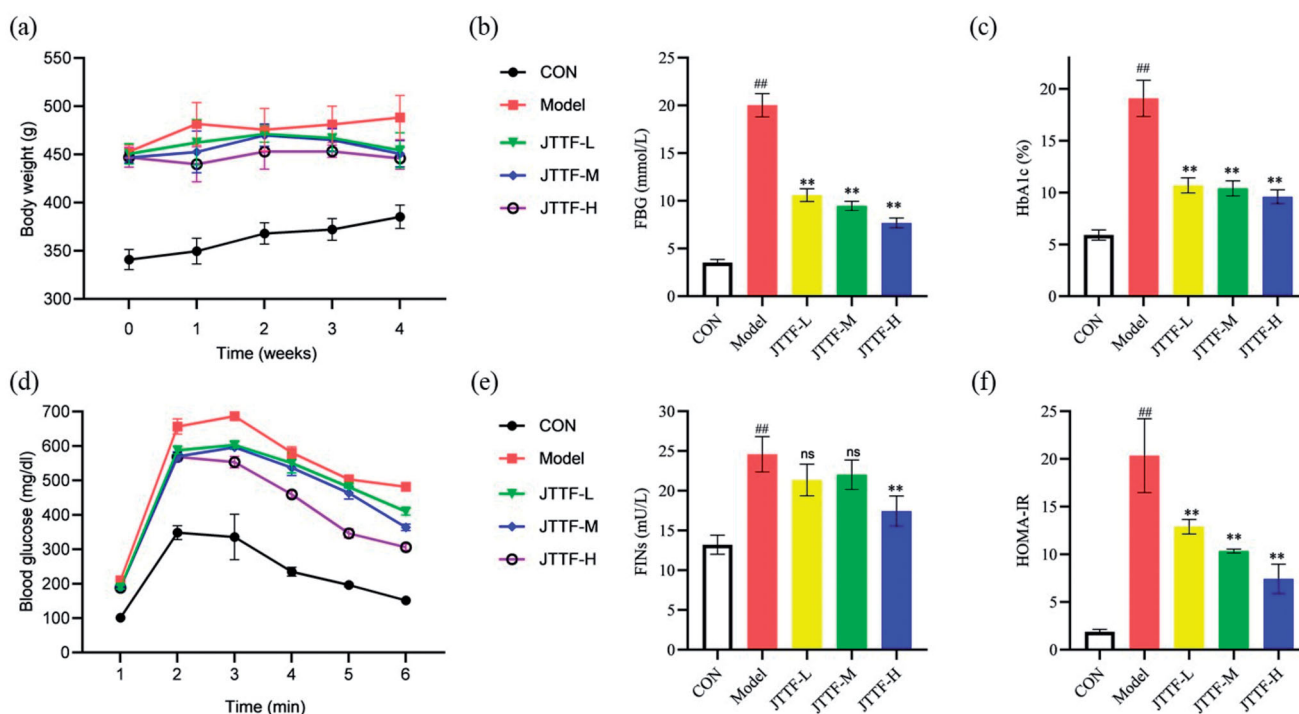
Figure 3. Effects of JTTF on body weight, FGB, HbA1c, IPGTT, FINs, and HOMA-IR in ZDF rats. (a) Body weight. (b) FBG. (c) HbA1c. (d) IPGTT. (e) FINs. (f) HOMA-IR. The data are expressed as the mean ± standard deviation, $^{\#}p < 0.05$ and $^{\#\#}p < 0.01$ were Model group compared with the control group; $^{*}p < 0.05$ and $^{**}p < 0.01$ were treatment groups compared with the Model group. FGB: fasting blood glucose; HbA1c: haemoglobin A1C; IPGTT: intraperitoneal glucose tolerance test; FINs: fasting serum insulin; HOMA-IR: homeostasis model assessment-insulin resistance.

greatest effect was observed for 200 μg/mL JTTF (Figure 8). Our study demonstrated that JTTF can alleviate the expression of inflammatory factors.

JTTF treatment reduced calcium release and ameliorated ERS

Next, we attempted to measure intracellular Ca^{2+} concentration in LPS-exposed INS-1 cells. As illustrated in Figure 9, Fluo-4 AM fluorescence intensity was increased in INS-1cells exposed to LPS. Conversely, treatment with all JTTF concentrations (50, 100, and 200 μg/mL), led to decreased Fluo-4 AM fluorescence intensity results across all treatment groups, thus demonstrating that the Ca^{2+} concentration gradually decreased with increasing JTTF concentration. HFD induced significant increases in levels of IRE1α and PERK in ZDF rats as compared to corresponding levels in the normal control. However, JTTF treatment induced a significant decrease in IRE1α and PERK levels as compared to corresponding levels in the model group, and the greatest decreases of IRE1α and PERK levels were observed for cells treated with 200 μg/mL JTTF. In addition, JTTF treatment drastically reduced protein levels of eIF2α, ATF6 and GRP78 as compared to their respective levels in the model group; eIF2α, ATF6 and GRP78 are master regulators of the UPR that normally occur in the ER of cells (Ibrahim et al. 2019). All of our results indicated that ERS was significantly attenuated by treatment with JTTF (Figure 10).

JTTF treatment down-regulated autophagy and decreased apoptosis in HFD rats

Consistently, we found that JTTF treatment reduced phosphorylation of mTOR. In addition, JTTF treatment reduced levels of

ULK1 and phospho-ULK1 in ZDF rats (Figure 11(a)). Beclin 1, a protein associated with gene expression involved in the formation of autophagosomes, may influence the rate of autophagy. Autophagy can be monitored using LC3 as a specific marker of autophagy and LC3II as a marker is highly correlated with autophagosome number. Therefore, to examine the role of Beclin 1 in autophagy, here we quantified expression levels of Beclin 1, p62, and LC3II/LC3I. Following JTTF treatment, a dose-dependent increase in p62 expression was observed that was accompanied by decreases of Beclin 1 and LC3II/LC3I levels (Figure 11(b)). In addition, autolysosomes significantly increased after treatment of LPS by AO dye staining analyses. As shown in Figure 10(c), excess autophagy induced by LPS could be inhibited by JTTF in INS-1 cells. The expression of Bax and CASPASE3 were significantly increased and the expression of Bcl-2 was decreased in ZDF rats. However, treatment with JTTF significantly increased the expression of Bcl-2, and reduced the expression of Bax and CASPASE3 in ZDF rats (Figure 12). These results suggested that JTTF could alleviate cell apoptosis.

JTTF treatment alleviated ERS and prevented excessive autophagy via the CaMKKβ/AMPK pathway

To investigate potential mechanisms by which JTTF treatment regulated the connection between ERS and autophagy, we monitored the activity of the CaMKKβ/AMPK signalling pathway. Our data revealed that JTTF decreased CAMKK activity and levels of phospho-CAMKKβ, as well as AMPK activity and levels of phospho-AMPK in HFD ZDF rats (Figure 13). Thus, JTTF may inhibit ERS and excessive autophagy by modulating CaMKKβ-AMPK pathway activity. Analog 5-aminoimidazole-4-carboxamide ribonucleotide (AICAR), as the agonist of the AMPK, could promote AMPK/ULK1/2 signalling axis in the regulation
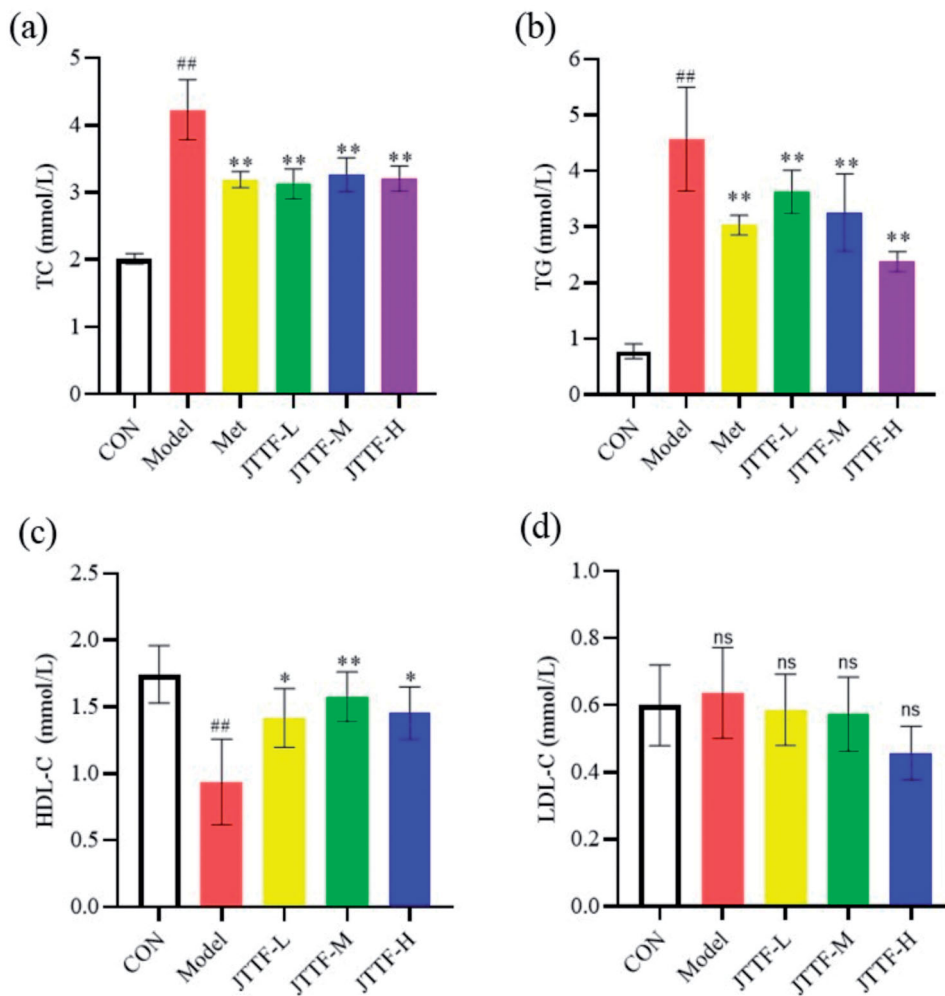
Figure 4. Effects of JTTF on serum lipid levels in ZDF rats. (a) TC. (b) TG. (c) HDL-C. (d) LDL-C. The data are expressed as the mean ± standard deviation, $^{\#}p < 0.05$ and $^{\#\#}p < 0.01$ were Model group compared with the control group; $^{*}p < 0.05$ and $^{**}p < 0.01$ were treatment groups compared with the Model group. TC: total cholesterol; TG: triglycerides; LDL-C: low-density lipoproteins, HDL-C: high-density lipoproteins.
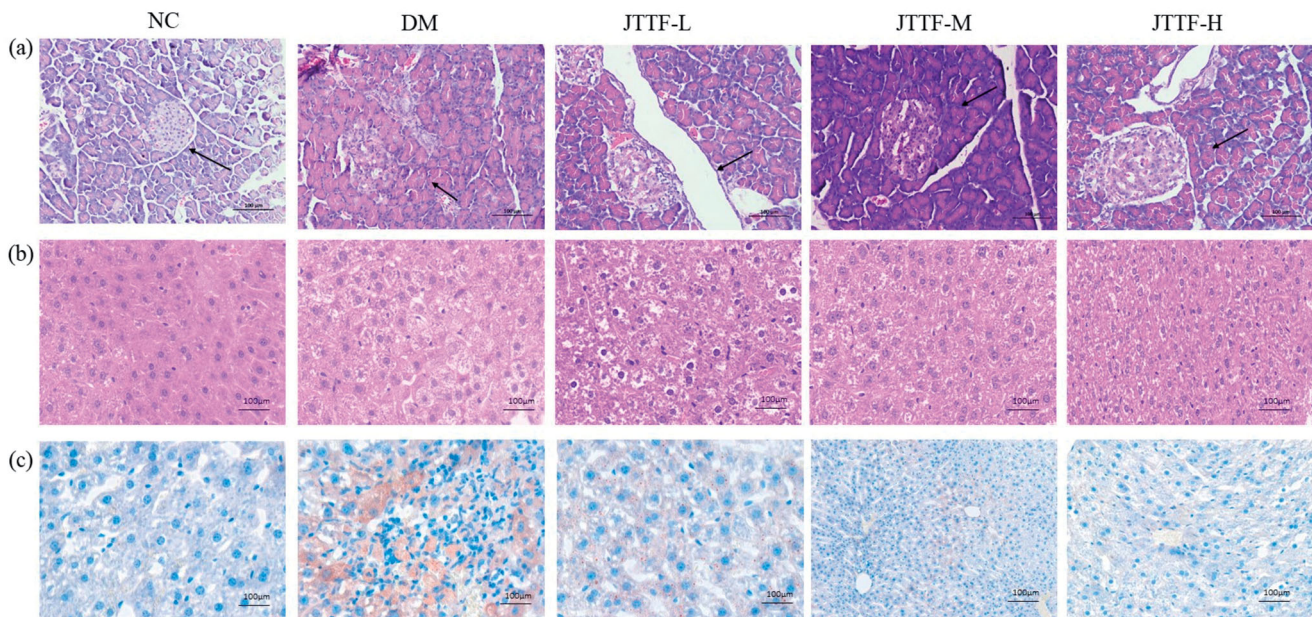

Figure 5. Histopathological examination of pancreas and liver histomorphology of ZDF rats of each group. (a) H&E staining of pancreas; (b) H&E staining of liver; (c) Oil red staining of liver.
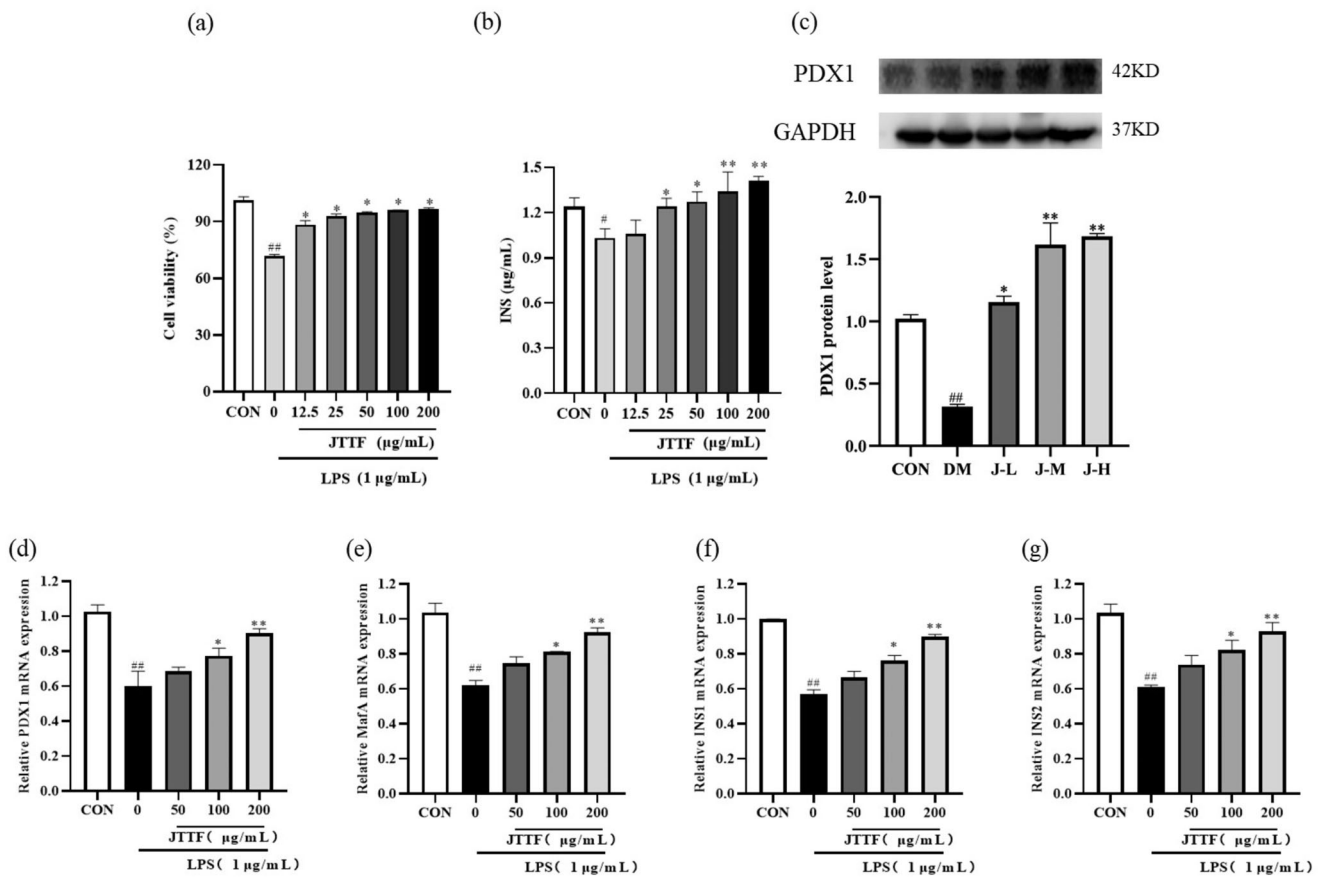
Figure 6. (a) The effects of JTTF with various concentrations on viability of INS-1 cells treated with LPS. #: compared with control group; *: compared with model group; *(#) and **(##) represent significance levels of $p < 0.05$ and $p < 0.01$, respectively. (b) The effects of JTTF with various concentrations on GSIS of INS-1 cells treated with LPS. #: compared with control group; *: compared with model group; *(#) and **(##) represent significance levels of $p < 0.05$ and $p < 0.01$, respectively. (c) Representative Western blot gel documents and summarised data on PDX1 in ZDF rats with different treatments. Quantitative analysis of protein. Bar graphs represent the means ± SD from five independent experiments. Compared with the control group, #$p < 0.05$; compared with the model group, *$p < 0.05$. (d), (e), (f), and (g) Representative PCR documents and summarised data on PDX1, MafA, INS1, and INS2 in INS-1 cells with different treatments. Quantitative analysis of protein. Bar graphs represent the means ± SD from five independent experiments. Compared with the control group, #$p < 0.05$; compared with the model group, *$p < 0.05$. GSIS: glucose-stimulated insulin secretion; PDX1: pancreatic duodenal homeobox-1; MafA: v-mafmusculoaponeurotic fibrosarcoma oncogene homologue A.
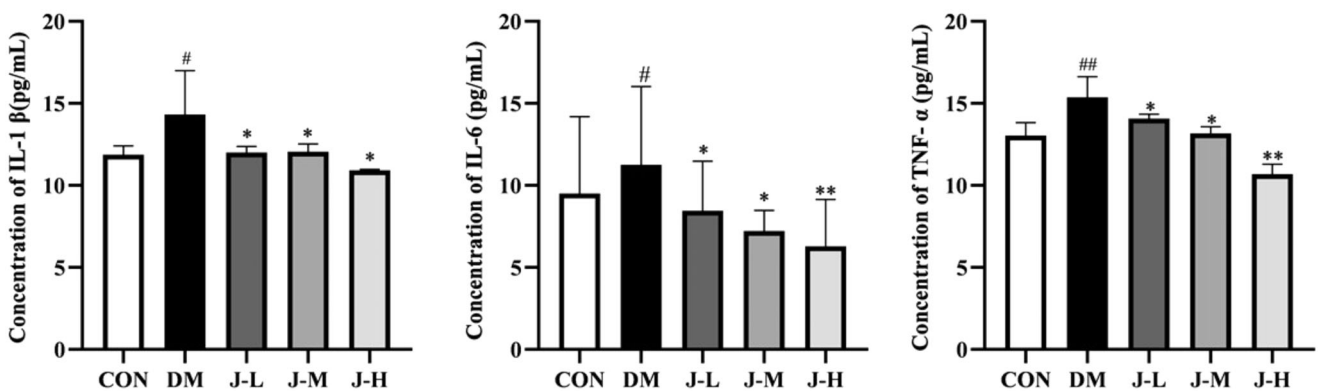

Figure 7. The effect on proinflammatory cytokine and chemokine with different concentration of JTTF. #: compared with control group; *: compared with model group; *(#) and **(##) represent significance levels of $p < 0.05$ and $p < 0.01$, respectively.

of autophagy (Knudsen et al. 2020). Protein levels of p-AMPK/ AMPK, LC3II/LC3I and Beclin 1 significantly increased in the AICAR group than in the control and model group. The JTTF-treated group showed a significantly reduced expression of p-AMPK/AMPK, LC3II/LC3I and Beclin 1 protein. Thus, JTTF may inhibit ERS and excessive autophagy by modulating CaMKKβ-AMPK pathway activity.

Discussion

Here, we found that JTTF relieved HFD-induced obesity and hyperglycaemia of ZDF rats, as well as improved LPS-induced ERS and autophagy of INS-1 cell demonstrate that the JTTF may have beneficial effects on T2DM. The major findings of the present study emphasise that JTTF reduced the release of Ca²⁺ in

(a)

(b)
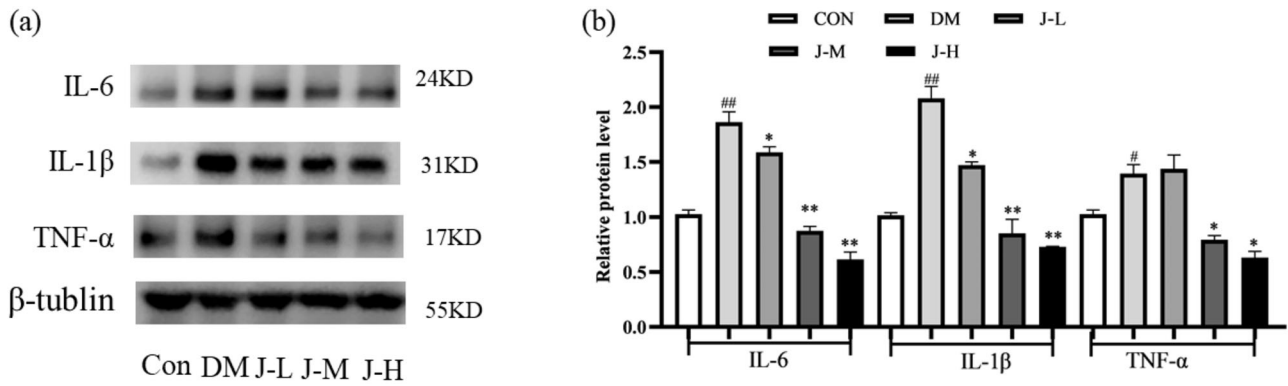
Figure 8. (a) Representative Western blot images showing levels of IL-6, IL-1β, and TNF-α proteins with or without JTTF treatment. (b) Quantitative analysis of protein. Bar graphs represent the means ± SD from four independent experiments. Compared with the control group, $^{\#}p < 0.05$, $^{\#\#}p < 0.01$; compared with the model group, $^{*}p < .05$, $^{**}p < .01$.
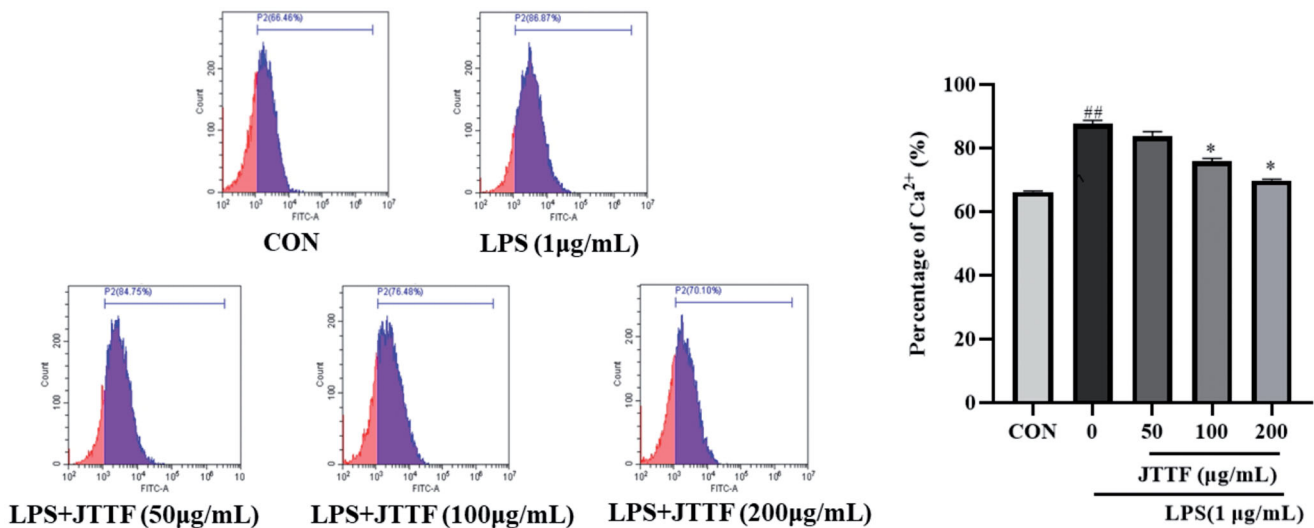

Figure 9. Effect of JTTF on INS-1 cells cytosolic Ca^{2+} concentration. P2 represents Fluo-4 AM-associated fluorescence intensity. Bar graph bars depict means ± SD from five independent experiments. Compared with the control group (without Fluo-4 AM), $^{\wedge} < 0.05$; Compared with the control group, $^{\#}p < 0.05$, $^{\#\#}p < 0.01$; compared with the model group, $^{*}p < 0.05$, $^{**}p < 0.01$.

INS-1 cells to ultimately alleviate ERS and prevent excessive autophagy, suggesting that JTTF is a promising therapeutic treatment for diabetes. Mechanistically, JTTF appeared to regulate diabetes-promoting ERS and excessive autophagy by modulating CAMKKβ/AMPK signalling pathway activity, one of the critical signal transduction pathways linking ERS to autophagy. Thus, our current results outline a novel therapeutic approach for use in developing more effective diabetes treatments.

PDX1 is an important transcription factor that regulates islet β-cell proliferation, differentiation, and function (Zhu et al. 2017). Reduced expression of PDX1 is thought to contribute to β-cell loss and dysfunction in diabetes (Fujimoto and Polonsky 2009). Decreased expression of PDX1 has been closely related to islet β-cell apoptosis induced by oxidative stress and ERS stress (Cnop et al. 2017). Furthermore, studies have found that restoring PDX1 protein levels can normalise β-cell mass by modulating β-cell survival under the diabetic condition (Claiborn et al. 2010). Thus, promoting PDX1 expression can be an effective strategy to preserve β-cell mass and function. In our study, PDX1 levels were consistently higher in JTTF treatment groups although ZL control group had higher PDX1 mRNA expression, indicating that JTTF may exhibit strong protective effects on islet β-cells by promoting PDX1 protein expression rather than

increasing the number of genes. However, further experimental experiments were demanded to validate the hypothesis.

Moderate ERS can protect β cells from damage by activating the UPR to preserve ER homeostasis (Kong et al. 2017). IR is countered by increased secretion of insulin during the development of diabetes. However, as insulin demand exceeds β-cell secretory capacity, the level of unfolded ER proteins in β-cells increase. Such sustained high-intensity stimulation can eventually trigger non-adaptive ERS and apoptotic responses (Fonseca et al. 2011; Walter and Ron 2011; Wang et al. 2018). In recent years, autophagy has been extensively studied, because of its role in regulating β-cell function and cell damage (Rivera et al. 2014). Under conditions, autophagy is key to maintaining β-cell function and survival by serving as an important mechanism for preventing β-cell failure (Hayes et al. 2017). In addition, autophagy plays an important role in maintaining both structural and functional integrity of the ER (Bernales et al. 2007), which are crucial for β-cell survival (Laybutt et al. 2007). Intriguingly, another study demonstrated that under diabetic conditions, upregulation of LC-3 and Beclin 1 expression after attenuation of PERK/eIF2a pathway activity could improve impaired autophagy (Fang et al. 2013). Meanwhile, endostatin-activated autophagic gene expression has been shown to alter XBP1 mRNA splicing via a
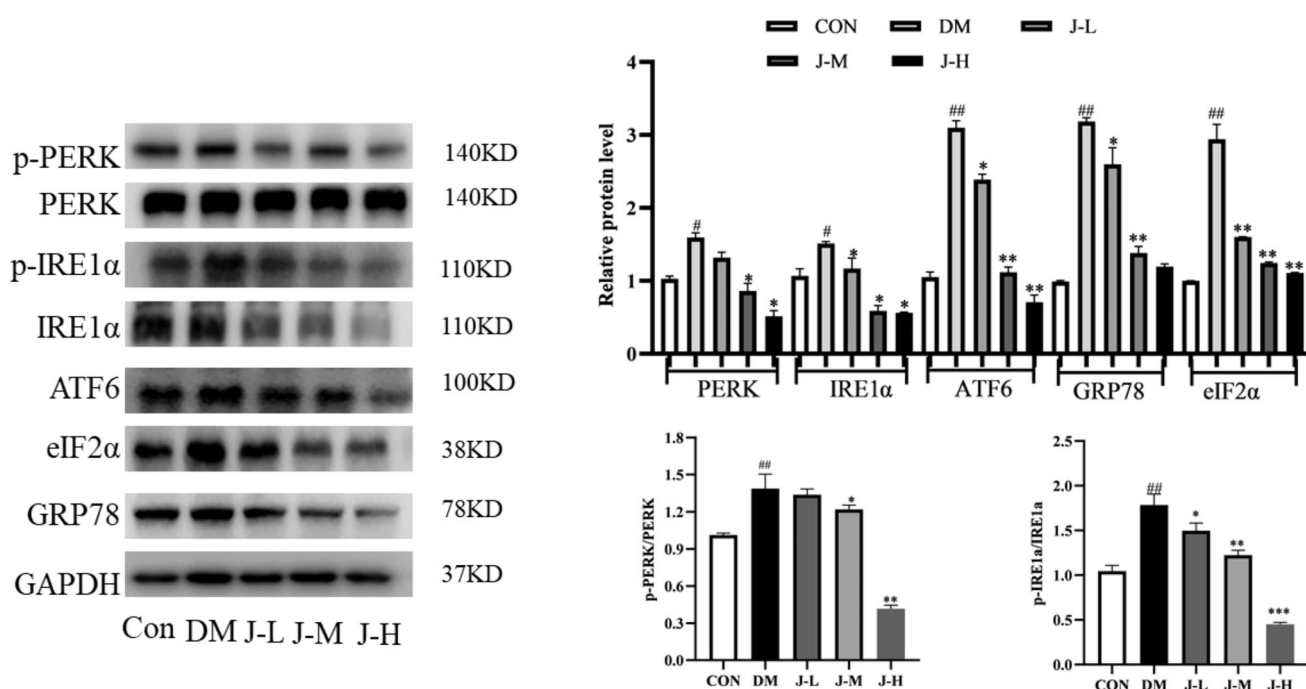
Figure 10. The effect of JTTF on levels of proteins in HFD ZDF rats. Representative Western blots showing expression of PERK, p-PERK, IRE1α, p- IRE1α, ATF6, eIF2α, and GRP78 proteins. Quantitative analysis of protein. Bar graph bars depict means ± SD from five independent experiments. Compared with the control group, [#]$p < 0.05$, [##]$p < 0.01$; compared with the model group, [*]$p < 0.05$, [**]$p < 0.01$.

mechanism involving IRE1α, with altered XBP1 mRNA splicing triggering an autophagic signal pathway linked to transcriptional regulation of Beclin 1 expression (Margariti et al. 2013). More recent research has revealed that in the presence of autophagy-stimulating factors such as IRE1α, UPR and ubiquitin-proteasome activities cannot adequately remove misfolded and unfolded proteins from the ER to prevent autophagy as long as stimulating factors are present (Qi and Chen 2019). Here we verified that JTTF treatment of HFD ZDF rats could decrease intracellular expression of PERK, p-PERK, IRE1α, p-IRE1α, ATF6, eIF2a, and GRP78 as compared to the model group. In addition, JTTF significantly increased cell viability and insulin secretion, as demonstrated using MTT assays and GSIS, as evidence for a cell-protective effect of JTTF treatment.

As for all endocrine diseases, including diabetes, autophagy appears to be beneficial or harmful, with the final outcome depends on the delicate balance between the amount of autophagy-triggering substrate and the capacity of autophagy machinery to remove the triggering substrate. Importantly, inflammation can regulate autophagy, while autophagy can shape the inflammatory response (Lapaquette et al. 2015). Autophagy is a dynamic and multistep process regulated by the ULK1 complex (Ravikumar et al. 2010). In our study, the model DM group had a higher level of Beclin1 than the normal group. Although the JTTF-L group had a slightly higher level of Beclin1 than the model group, the JTTF-H group and JTTF-M had a significantly lower level of Beclin1 and LC3 than the model DM group. This may be related to the JTTF dose-dependence and needs further study. Therefore, it could be expected that JTTF could decrease the level of Beclin1/LC3 to protect the islet cells by suppressing excessive autophagy.

The cellular stress response would lead to decreased ATP concentration with concomitantly increased AMP concentration that together increase the intracellular AMP/ATP ratio, triggering AMPK activation (Motoshima et al. 2006; Gwinn et al. 2008).

Importantly, AMPK can also be activated by upstream CaMKKβ kinases (Maeda et al. 2018). AMPK/mTOR pathway, as a potent regulator, opposes each other to regulate ULK1 complex activity, with phosphorylation of AMPK previously shown to positively regulate autophagy by regulating downstream signalling molecules (Hardie 2011; Sanli et al. 2014). Importantly, earlier research had shown that AMPK binds and phosphorylates ULK1 that then triggers downstream signals to induce autophagy, while mTOR could inhibit autophagy to promote cell growth and proliferation (Nojima et al. 2003). Meanwhile, mTORC1 has been shown to inhibit ULK1 activation and interrupting its interaction with AMPK (Egan et al. 2011; Kim et al. 2011), while activation of AMPK signalling and inhibition of mTORC1 activity decreased phosphorylation of ULK1 under hyperglycaemia condition (Zhou et al. 2019). Based on these results, here we further used AMPK activators to assess AMPK signalling pathway activity, showing that treatment with AICAR effectively activated LPS-induced AMPK, thereby inhibiting β-cell excessive autophagy through JTTF treatment. Collectively, these results provide new insights to enhance our understanding of mechanisms of pancreatic dysfunction by showing that JTTF treatment acts via the AMPK/mTOR pathway to prevent excessive autophagy and maintain appropriate autophagy.

ERS causes misfolding of the ER cavity and aggregation of unfolded proteins, both of which disrupt homeostatic control of calcium ion levels (Wang et al. 2013). As activation of CaMKKβ is primarily dependent on conformational protein structural changes induced by binding of Ca^{2+} and calmodulin, the level of free cytoplasmic Ca^{2+} is an essential requirement for subsequent activation of CaMKKβ (Hassan et al. 2016; Yin et al. 2018). Moreover, we found that increased Ca^{2+} level activated CaMKKβ by showing that LPS exposure, which increases Ca^{2+} concentration, leading to CaMKKβ activation. However, ERS, or excessive Ca^{2+} can cause excessive autophagy, a state whereby autophagosomes formation exceeds lysosomal degradation
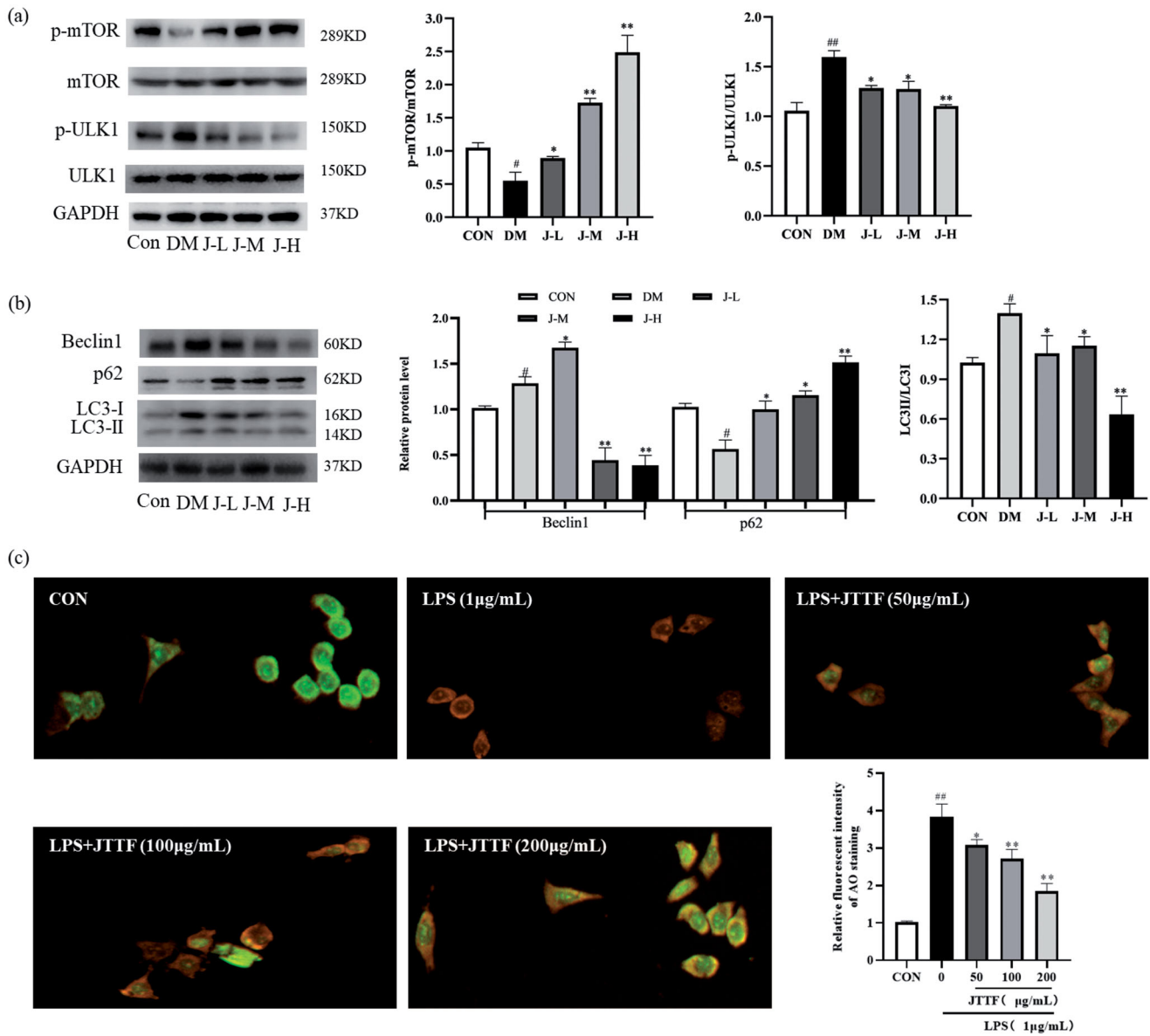
Figure 11. (a and b) JTTF restored excessive autophagy in HFD ZDF rats. Representative Western blot images and summarised data of mTOR, p-mTOR, ULK1, p-ULK,1 Beclin 1, p62, and LC3 levels in different treatments. Quantitative analysis of protein. Bar graph bars depict means ± SD from five independent experiments. Compared with the control group, $^\#p < 0.05$, $^{\#\#}p < 0.01$; compared with the model group, $^*p < 0.05$, $^{**}p < 0.01$. (c) AO dye staining for autophagic vacuoles was carried out in INS-1 cells which were treated with LPS in all JTTF concentrations (50, 100, and 200 μg/mL) JTTF. Cells were immediately analysed by fluorescence microscopy and quantified. mTOR: mammalian target of rapamycin; ULK1: UNC-51-like kinase 1; LC3: microtubule-associated protein.
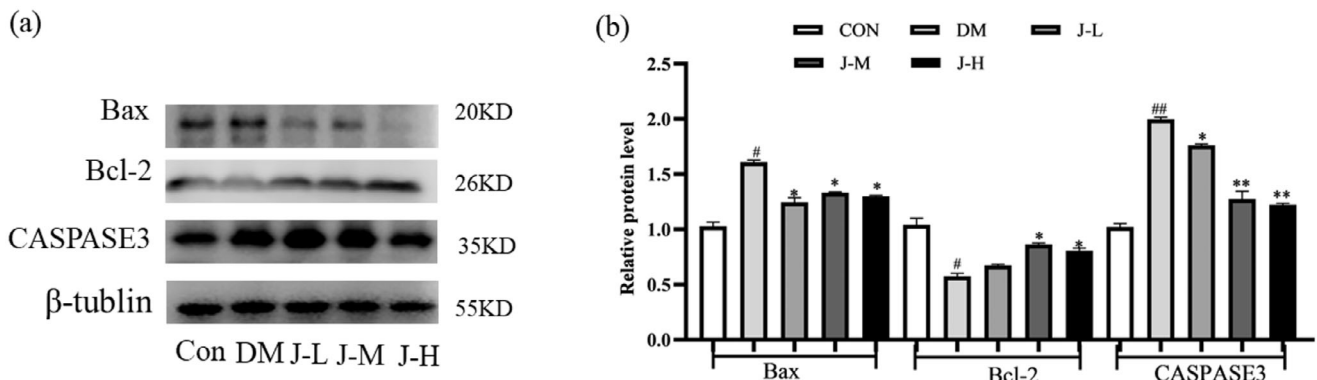
Figure 12. (a) Western blot and quantified protein expression levels of Bax, Bcl-2, CASPASE3 and β-tublin. (b) Bar graph bars depict means ± SD from five independent experiments. Compared with the control group, $^\wedge p < 0.05$; Compared with the control group, $^\#p < 0.05$, $^{\#\#}p < 0.01$; compared with the model group, $^*p < 0.05$, $^{**}p < 0.01$. Bax: BCL2-Associated X; Bcl-2: B-cell lymphoma-2.
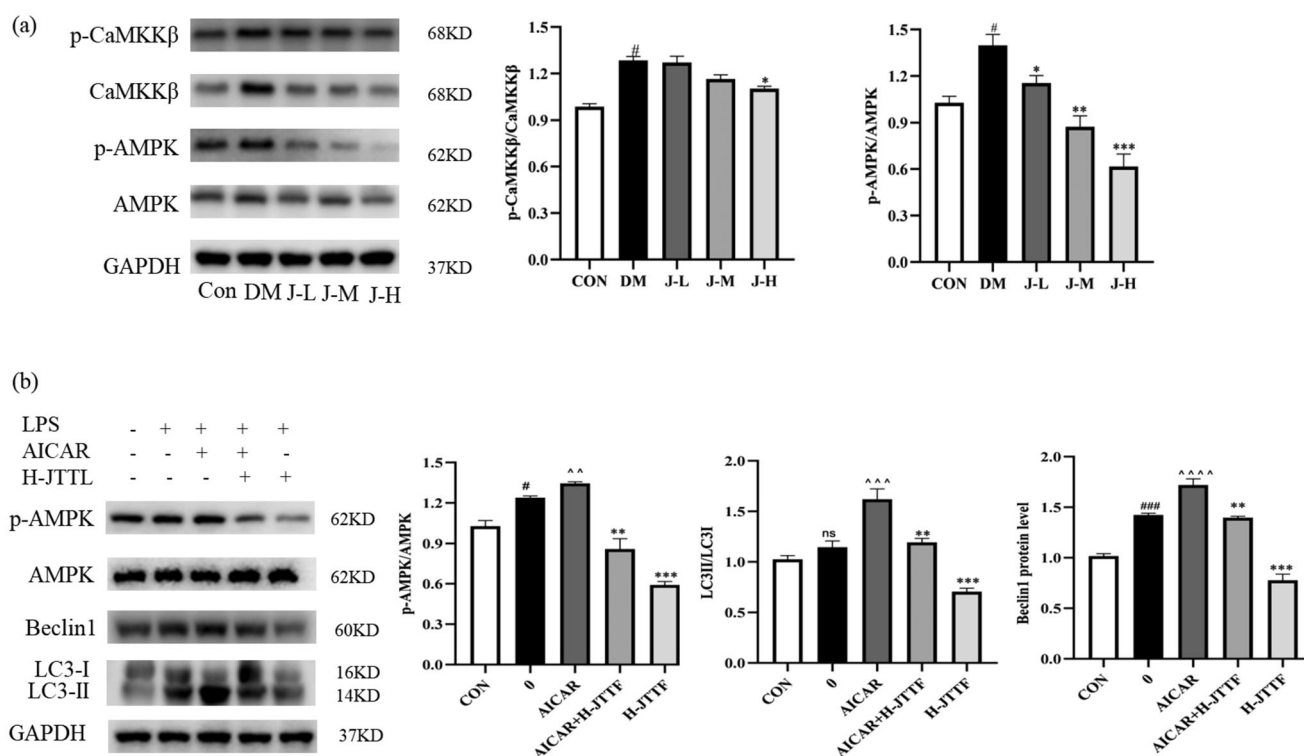
Figure 13. (a) Representative Western blots showing protein levels of CaMKKβ, p-CaMKKβ, AMPK, and p-AMPK in HFD ZDF rats. (b) JTTF inhibited AICAR-induced AMPK activation and autophagy, representative Western blots showing protein levels of AMPK, p-AMPK, Beclin 1, and LC3 levels in INS-1 cells. Quantitative analysis of protein levels. Bar graph bars depict means ± SD from three independent experiments. Compared with the control group, $^{\#}p < 0.05$, $^{\#\#}p < 0.01$; compared with the model group, $^{*}p < 0.05$, $^{**}p < 0.01$. CaMKKβ: Ca^{2+}/Calmodulin-dependent protein kinase kinase; AMPK: AMP-activated protein kinase; AICAR: analog 5-aminoimidazole-4-carboxamide ribonucleotide.

capacity, resulting in cell death (Ma et al. 2011). In this study, we confirmed that JTTF downregulated excessive autophagy and repressed ERS by inhibiting the CaMKKβ/AMPK/mTOR/ULK1 pathway.

ERS directly regulates autophagy through UPR pathway-associated proteins PERK, IRE1α, and ATF6 (Kouroku et al. 2007), while also indirectly regulating autophagy by altering intracytoplasmic Ca^{2+} concentration. In addition, autophagy can also synergistically regulate ERS to either restore cell stability or promote cell death, underscoring the potential of regulatory targets common to both ERS and autophagy pathways to serve as a foundation for future development of novel diabetes treatments. In fact, appropriate ERS and autophagy work together to exert independent cytoprotective effects by participating in a coordinated interaction that promotes cell survival. However, after cells are subjected to continual high-intensity stress, the coordinated and protective interaction between ERS and autophagy becomes an unbalanced and destructive interaction, leading to cell damage and even cell death.

Conclusions

Our study demonstrated the mechanism whereby JTTF treatment protects against pancreatic β-cell injury. Notably, JTTF treatment led to reduced apoptosis of pancreatic β-cells via a putative mechanism involving decreased ERS and autophagic activity. JTTF protective effects against cell damage in HFD ZDF rats and LPS-exposed INS-1 cell-based diabetes model result from inhibition of ERS and excessive autophagy due to JTTF modulation of CaMKKβ/AMPK signalling pathway activity. Therefore, JTTF displayed positive effects in the treatment of diabetes and the

mechanism of its anti-diabetes activity was initially investigated, which related to suppressing excessive autophagy and ERS. However, there are also some limitations. (i) The underlying mechanism by which active ingredients of JTTF balance autophagy and ERS remains unclear; (ii) the active ingredients screened might be inconsistent with the ingredients actually absorbed in the blood of the diabetic rats. Thus, *in vivo* and *in vitro* verifications of active ingredients are needed for further evaluation.

Informed consent

The manuscript is approved by all authors for publication.

Author contributions

Conceived and designed the experiments: Chunli Piao and Liwei Sun; Performed the experiments: Jinli Luo and Wenqi Jin; Analysed the data: Jinli Luo, Wenqi Jin and Meiying Jin; Contributed reagents/materials/analysis tools: Weiwei Pan, Shengnan Gao Xiaohua Zhao, and Xingrong Lai; Wrote the paper: Jinli Luo.

Disclosure statement

No potential conflict of interest was reported by the author(s).

Funding

Data availability statement

The data and materials generated or analysed during this study are available from the corresponding author on reasonable request.

References

Alers S, Löffler AS, Wesselborg S, Stork B. 2012. Role of AMPK-mTOR-Ulk1/2 in the regulation of autophagy: cross talk, shortcuts, and feedbacks. Mol Cell Biol. 32(1):2–11.

Berbudi A, Rahmadika N, Tjahjadi AI, Ruslami R. 2020. Type 2 diabetes and its impact on the immune system. Curr Diabetes Rev. 16(5):442–449.

Bernales S, Schuck S, Walter P. 2007. ER-phagy: selective autophagy of the endoplasmic reticulum. Autophagy. 3(3):285–287.

Cheng SW, Fryer LG, Carling D, Shepherd PR. 2004. Thr2446 is a novel mammalian target of rapamycin (mTOR) phosphorylation site regulated by nutrient status. J Biol Chem. 279(16):15719–15722.

Cho NH, Shaw JE, Karuranga S, Huang Y, da Rocha Fernandes JD, Ohlrogge AW, Malanda B. 2018. IDF Diabetes Atlas: global estimates of diabetes prevalence for 2017 and projections for 2045. Diabetes Res Clin Pract. 138:271–281.

Claiborn KC, Sachdeva MM, Cannon CE, Groff DN, Singer JD, Stoffers DA. 2010. Pcif1 modulates Pdx1 protein stability and pancreatic β cell function and survival in mice. J Clin Invest. 120(10):3713–3721.

Cnop M, Toivonen S, Igoillo-Esteve M, Salpea P. 2017. Endoplasmic reticulum stress and eIF2α phosphorylation: The Achilles heel of pancreatic β cells. Mol Metab. 6(9):1024–1039.

Dai H, Liu F, Qiu X, Liu W, Dong Z, Jia Y, Feng Z, Liu Z, Zhao Q, Gao Y, et al. 2020. Alleviation by Mahuang Fuzi and Shenzhuo decoction in high glucose-induced podocyte injury by inhibiting the activation of Wnt/β-catenin signaling pathway, resulting in activation of podocyte autophagy. Evid Based Complement Alternat Med. 2020:7809427.

Dong X, Zeng Y, Liu Y, You L, Yin X, Fu J, Ni J. 2020. Aloe-emodin: a review of its pharmacology, toxicity, and pharmacokinetics. Phytother Res. 34(2):270–281.

Egan DF, Shackelford DB, Mihaylova MM, Gelino S, Kohnz RA, Mair W, Vasquez DS, Joshi A, Gwinn DM, Taylor R, et al. 2011. Phosphorylation of ULK1 (hATG1) by AMP-activated protein kinase connects energy sensing to mitophagy. Science. 331(6016):456–461.

Fang L, Zhou Y, Cao H, Wen P, Jiang L, He W, Dai C, Yang J. 2013. Autophagy attenuates diabetic glomerular damage through protection of hyperglycemia-induced podocyte injury. PLoS One. 8(4):e60546.

Feng N, Wang B, Cai P, Zheng W, Zou H, Gu J, Yuan Y, Liu X, Liu Z, Bian J. 2020. ZEA-induced autophagy in TM4 cells was mediated by the release of Ca²⁺ activates CaMKKβ-AMPK signaling pathway in the endoplasmic reticulum. Toxicol Lett. 323:1–9.

Fonseca SG, Gromada J, Urano F. 2011. Endoplasmic reticulum stress and pancreatic β-cell death. Trends Endocrinol Metab. 22(7):266–274.

Fujimoto K, Polonsky KS. 2009. Pdx1 and other factors that regulate pancreatic beta-cell survival. Diabetes Obes Metab. 11 Suppl 4:30–37.

Green MF, Anderson KA, Means AR. 2011. Characterization of the CaMKKβ-AMPK signaling complex. Cell Signal. 23(12):2005–2012.

Gwinn DM, Shackelford DB, Egan DF, Mihaylova MM, Mery A, Vasquez DS, Turk BE, Shaw RJ. 2008. AMPK phosphorylation of raptor mediates a metabolic checkpoint. Mol Cell. 30(2):214–226.

Hardie DG. 2011. AMPK and autophagy get connected. Embo J. 30(4): 634–635.

Hashemzaei M, Entezari Heravi R, Rezaee R, Roohbakhsh A, Karimi G. 2017. Regulation of autophagy by some natural products as a potential therapeutic strategy for cardiovascular disorders. Eur J Pharmacol. 802: 44–51.

Hassan H, Tian X, Inoue K, Chai N, Liu C, Soda K, Moeckel G, Tufro A, Lee AH, Somlo S, et al. 2016. Essential role of X-Box binding protein-1 during endoplasmic reticulum stress in podocytes. J Am Soc Nephrol. 27(4):1055–1065.

Hayes HL, Peterson BS, Haldeman JM, Newgard CB, Hohmeier HE, Stephens SB. 2017. Delayed apoptosis allows islet β-cells to implement an autophagic mechanism to promote cell survival. PLoS One. 12(2): e0172567.

Holland AM, Hale MA, Kagami H, Hammer RE, MacDonald RJ. 2002. Experimental control of pancreatic development and maintenance. Proc Natl Acad Sci USA. 99(19):12236–12241.

Huang L, Lu FE, Yang XY. 2008. [Effects of huanglian jiedu decoction on the oxidative stress of liver mitochondria in insulin resistant rats]. Zhongguo Zhong Xi Yi Jie He Za Zhi. 28(8):725–728. Chinese.

Hussain A, Cho JS, Kim JS, Lee YI. 2021. Protective effects of polyphenol enriched complex plants extract on metabolic dysfunctions associated with obesity and related nonalcoholic fatty liver diseases in high fat diet-Induced C57BL/6 Mice. Molecules (Basel, Switzerland). 26(2):302.

Ibrahim IM, Abdelmalek DH, Elfiky AA. 2019. GRP78: A cell's response to stress. Life Sci. 226:156–163.

Jia Q, Zhu R, Tian Y, Chen B, Li R, Li L, Wang L, Che Y, Zhao D, Mo F, et al. 2019. Salvia miltiorrhiza in diabetes: a review of its pharmacology, phytochemistry, and safety. Phytomedicine. 58:152871.

Jiang XT, Piao CL, Mi J, Jin MY, Liu XR, Pan WW. 2018. Effects of Jiedu Tongluo Tiaogan Formula on the endoplasmic reticulum stress and inflammation of adipocytes. J Beijing Univ Traditional Chin Med. 41:1012–1018+1024. Chinese.

Jin MY, Piao CL, Pan WW, Wang ML. 2020. Clinical observation of Jiedu Tongluo Tiaogan Formula combined with abdominal acupuncture in the treatment of obesity type 2 diabetes mellitus (phlegm stasis blocking collaterals). Cardiovasc Dis Electronic J Integr Traditional Chin Western Med. 8:169–170. Chinese.

Kim J, Kundu M, Viollet B, Guan KL. 2011. AMPK and mTOR regulate autophagy through direct phosphorylation of Ulk1. Nat Cell Biol. 13(2): 132–141.

Knudsen JR, Madsen AB, Persson KW, Henríquez-Olguín C, Li Z, Jensen TE. 2020. The ULK1/2 and AMPK inhibitor SBI-0206965 blocks AICAR and insulin-stimulated glucose transport. IJMS. 21(7):2344.

Kong FJ, Wu JH, Sun SY, Zhou JQ. 2017. The endoplasmic reticulum stress/autophagy pathway is involved in cholesterol-induced pancreatic β-cell injury. Sci Rep. 7:44746.

Kouroku Y, Fujita E, Tanida I, Ueno T, Isoai A, Kumagai H, Ogawa S, Kaufman RJ, Kominami E, Momoi T. 2007. ER stress (PERK/eIF2alpha phosphorylation) mediates the polyglutamine-induced LC3 conversion, an essential step for autophagy formation. Cell Death Differ. 14(2):230–239.

Lamm N, Rogers S, Cesare AJ. 2019. The mTOR pathway: implications for DNA replication. Prog Biophys Mol Biol. 147:17–25.

Lapaquette P, Guzzo J, Bretillon L, Bringer MA. 2015. Cellular and molecular connections between autophagy and inflammation. Mediators Inflamm. 2015:398483.

Laybutt DR, Preston AM, Akerfeldt MC, Kench JG, Busch AK, Biankin AV, Biden TJ. 2007. Endoplasmic reticulum stress contributes to beta cell apoptosis in type 2 diabetes. Diabetologia. 50(4):752–763.

Lei K, Davis RJ. 2003. JNK phosphorylation of Bim-related members of the Bcl2 family induces Bax-dependent apoptosis. Proc Natl Acad Sci USA. 100(5):2432–2437.

Leng Y, Zhou X, Xie Z, Hu Z, Gao H, Liu X, Xie H, Fu X, Xie C. 2020. Efficacy and safety of Chinese herbal medicine on blood glucose fluctuations in patients with type 2 diabetes mellitus: a protocol of systematic review and meta-analysis. Medicine (Baltimore). 99(34):e21904.

Li S, Li H, Yang D, Yu X, Irwin DM, Niu G, Tan H. 2017. Excessive autophagy activation and increased apoptosis are associated with palmitic acid-induced cardiomyocyte insulin resistance. J Diabetes Res. 2017:2376893.

Liao J, Zang J, Yuan F, Liu S, Zhang Y, Li H, Piao Z, Li H. 2016. Identification and analysis of anthocyanin components in fruit color variation in Schisandra chinensis. J Sci Food Agric. 96(9):3213–3219.

Liao Y, Duan B, Zhang Y, Zhang X, Xia B. 2019. Excessive ER-phagy mediated by the autophagy receptor FAM134B results in ER stress, the unfolded protein response, and cell death in HeLa cells. J Biol Chem. 294(52):20009–20023.

Liu J, Yang R, Meng H, Zhou T, He Q. 2020. In vitro treatment of 3 T3-L1 adipocytes with recombinant calcium/calmodulin-dependent Protein Kinase IV (CaMKIV) limits ER stress and improves insulin sensitivity through inhibition of autophagy via the mTOR/CREB signaling pathway. BMC Endocr Disord. 20(1):104.

Liu Y, Song A, Zang S, Wang C, Song G, Li X, Zhu Y, Yu X, Li L, Wang Y, et al. 2015. Jinlida reduces insulin resistance and ameliorates liver oxidative stress in high-fat fed rats. J Ethnopharmacol. 162:244–252.

Liu Z, Wang W, Luo J, Zhang Y, Zhang Y, Gan Z, Shen X, Zhang Y, Meng X. 2021. Anti-apoptotic role of sanhuang xiexin decoction and anisodamine in endotoxemia. Front Pharmacol. 12:531325.

Lontchi-Yimagou E, Sobngwi E, Matsha TE, Kengne AP. 2013. Diabetes mellitus and inflammation. Curr Diab Rep. 13(3):435–444.

Ma H, Guo R, Yu L, Zhang Y, Ren J. 2011. Aldehyde dehydrogenase 2 (ALDH2) rescues myocardial ischaemia/reperfusion injury: role of autophagy paradox and toxic aldehyde. Eur Heart J. 32(8):1025–1038.

Maeda A, Shirao T, Shirasaya D, Yoshioka Y, Yamashita Y, Akagawa M, Ashida H. 2018. Piperine promotes glucose uptake through ROS-dependent activation of the CAMKK/AMPK signaling pathway in skeletal muscle. Mol Nutr Food Res. 62(11):e1800086.

Margariti A, Li H, Chen T, Martin D, Vizcay-Barrena G, Alam S, Karamariti E, Xiao Q, Zampetaki A, Zhang Z, et al. 2013. XBP1 mRNA splicing triggers an autophagic response in endothelial cells through BECLIN-1 transcriptional activation. J Biol Chem. 288(2):859–872.

Motoshima H, Goldstein BJ, Igata M, Araki E. 2006. AMPK and cell proliferation–AMPK as a therapeutic target for atherosclerosis and cancer. J Physiol. 574(Pt 1):63–71.

Nojima H, Tokunaga C, Eguchi S, Oshiro N, Hidayat S, Yoshino K, Hara K, Tanaka N, Avruch J, Yonezawa K. 2003. The mammalian target of rapamycin (mTOR) partner, raptor, binds the mTOR substrates p70 S6 kinase and 4E-BP1 through their TOR signaling (TOS) motif. J Biol Chem. 278(18):15461–15464.

Ogurtsova K, da Rocha Fernandes JD, Huang Y, Linnenkamp U, Guariguata L, Cho NH, Cavan D, Shaw JE, Makaroff LE. 2017. IDF Diabetes Atlas: global estimates for the prevalence of diabetes for 2015 and 2040. Diabetes Res Clin Pract. 128:40–50.

Ozcan U, Yilmaz E, Ozcan L, Furuhashi M, Vaillancourt E, Smith RO, Görgün CZ, Hotamisligil GS. 2006. Chemical chaperones reduce ER stress and restore glucose homeostasis in a mouse model of type 2 diabetes. Science. 313(5790):1137–1140.

Qi Z, Chen L. 2019. Endoplasmic reticulum stress and autophagy. Adv Exp Med Biol. 1206:167–177.

Ravikumar B, Sarkar S, Davies JE, Futter M, Garcia-Arencibia M, Green-Thompson ZW, Jimenez-Sanchez M, Korolchuk VI, Lichtenberg M, Luo S, et al. 2010. Regulation of mammalian autophagy in physiology and pathophysiology. Physiol Rev. 90(4):1383–1435.

Ren XD, Zhang YW, Wang XP, Li YR. 2017. Effects of Dangguibuxue decoction on rat glomerular mesangial cells cultured under high glucose conditions. BMC Complement Altern Med. 17(1):283.

Rivera JF, Costes S, Gurlo T, Glabe CG, Butler PC. 2014. Autophagy defends pancreatic β cells from human islet amyloid polypeptide-induced toxicity. J Clin Invest. 124(8):3489–3500.

Sanli T, Steinberg GR, Singh G, Tsakiridis T. 2014. AMP-activated protein kinase (AMPK) beyond metabolism: a novel genomic stress sensor participating in the DNA damage response pathway. Cancer Biol Ther. 15(2):156–169.

Sciarretta S, Yee D, Nagarajan N, Bianchi F, Saito T, Valenti V, Tong M, Del Re DP, Vecchione C, Schirone L, et al. 2018. Trehalose-induced activation of autophagy improves cardiac remodeling after myocardial infarction. J Am Coll Cardiol. 71(18):1999–2010.

Shi Y, Pan D, Yan L, Chen H, Zhang X, Yuan J, Mu B. 2020. Salvianolic acid B improved insulin resistance through suppression of hepatic ER stress in ob/ob mice. Biochem Biophys Res Commun. 526(3):733–737.

Shoelson SE, Lee J, Goldfine AB. 2006. Inflammation and insulin resistance. J Clin Invest. 116(7):1793–1801.

Song YM, Lee YH, Kim JW, Ham DS, Kang ES, Cha BS, Lee HC, Lee BW. 2015. Metformin alleviates hepatosteatosis by restoring SIRT1-mediated autophagy induction via an AMP-activated protein kinase-independent pathway. Autophagy. 11(1):46–59.

Stoffers DA, Zinkin NT, Stanojevic V, Clarke WL, Habener JF. 1997. Pancreatic agenesis attributable to a single nucleotide deletion in the human IPF1 gene coding sequence. Nat Genet. 15(1):106–110.

Thomé MP, Filippi-Chiela EC, Villodre ES, Migliavaca CB, Onzi GR, Felipe KB, Lenz G. 2016. Ratiometric analysis of acridine orange staining in the study of acidic organelles and autophagy. J Cell Sci. 129:4622–4632.

Walter P, Ron D. 2011. The unfolded protein response: from stress pathway to homeostatic regulation. Science. 334(6059):1081–1086.

Wang CL, Liu C, Niu LL, Wang LR, Hou LH, Cao XH. 2013. Surfactin-induced apoptosis through ROS-ERS-Ca²⁺-ERK pathways in HepG2 cells. Cell Biochem Biophys. 67(3):1433–1439.

Wang Q, You T, Fan H, Wang Y, Chu T, Poncz M, Zhu L. 2017. Rapamycin and bafilomycin A1 alter autophagy and megakaryopoiesis. Platelets. 28(1):82–89.

Wang W, Chen Q, Yang X, Wu J, Huang F. 2020. Sini decoction ameliorates interrelated lung injury in septic mice by modulating the composition of gut microbiota. Microb Pathog. 140:103956.

Wang X, Gao L, Lin H, Song J, Wang J, Yin Y, Zhao J, Xu X, Li Z, Li L. 2018. Mangiferin prevents diabetic nephropathy progression and protects podocyte function via autophagy in diabetic rat glomeruli. Eur J Pharmacol. 824:170–178.

Watada H, Fujitani Y. 2015. Minireview: autophagy in pancreatic β-cells and its implication in diabetes. Mol Endocrinol. 29(3):338–348.

Xiao B, Sanders MJ, Carmena D, Bright NJ, Haire LF, Underwood E, Patel BR, Heath RB, Walker PA, Hallen S, et al. 2013. Structural basis of AMPK regulation by small molecule activators. Nat Commun. 4:3017.

Xiong XJ. 2020. [Gegen Qinlian decoction formula syndrome and its application in diabetes, hypertension, hyperlipidemia and obesity]. Zhongguo Zhong Yao Za Zhi. 45(12):2760–2764. Chinese.

Yin H, Zhao L, Wang Y, Li S, Huo H, Chen H. 2018. Duck enteritis virus activates CaMKKβ-AMPK to trigger autophagy in duck embryo fibroblast cells via increased cytosolic calcium. Virol J. 15(1):120.

Zhang Q, Piao C, Jin W, Jin D, Wang H, Tang C, Zhao X, Zhang N, Gao S, Lian F. 2021. Decoding the chemical composition and pharmacological mechanisms of Jiedu Tongluo Tiaogan Formula using high-performance liquid chromatography coupled with network pharmacology-based investigation. Aging (Albany NY). 13(21):24290–24312.

Zhou D, Zhou M, Wang Z, Fu Y, Jia M, Wang X, Liu M, Zhang Y, Sun Y, Zhou Y, et al. 2019. Progranulin alleviates podocyte injury via regulating CAMKK/AMPK-mediated autophagy under diabetic conditions. J Mol Med (Berl). 97(11):1507–1520.

Zhu Y, Liu Q, Zhou Z, Ikeda Y. 2017. PDX1, Neurogenin-3, and MAFA: critical transcription regulators for beta cell development and regeneration. Stem Cell Res Ther. 8(1):240.